Radiation in Art and Archeometry

Edited by

D.C. Creagh

Faculty of Information Science and Engineering
Division of Management and Technology
University of Canberra
Canberra
Australia

and

D.A. Bradley

School of Physics
University of Exeter
Exeter
United Kingdom

ELSEVIER
2000
Amsterdam - Lausanne - New York - Oxford - Shannon - Singapore - Tokyo

ELSEVIER SCIENCE B.V.
Sara Burgerhartstraat 25
P.O. Box 211, 1000 AE Amsterdam, The Netherlands

First edition 2000

Library of Congress Cataloging in Publication Data
A catalog record from the Library of Congress has been applied for.

ISBN: 0 444 50487 7

♾ The paper used in this publication meets the requirements of ANSI/NISO Z39.48-1992 (Permanence of Paper).
Printed in The Netherlands.

Radiation in Art and Archeometry
D.C. Creagh and D.A. Bradley (editors)

A Synchrotron X-ray diffraction study of Egyptian cosmetics

P. Martinetto[a,b], M. Anne[c], E. Dooryhée[b], G. Tsoucaris[a], Ph. Walter[a]

[a]Laboratoire de recherche des musées de France, UMR 171 du C.N.R.S.,
6, rue des Pyramides, F-75041 Paris Cedex 1, France

[b]European Synchrotron Radiation Facility, 6, rue Jules Horowitz, B.P. 220, F-38043
Grenoble Cedex, France

[c]Laboratoire de Cristallographie - CNRS, 25, avenue des Martyrs - BP 166,
F-38042 Grenoble Cedex 9, France

1. INTRODUCTION

1.1. Archaeological background

Visitors of the Egyptian collections are amazed to see the amount and the exceptional preservation of the everyday life artefacts, and note the abundance of the toilet accessories. Unguents, creams, powders and eye-paints were commonly used and kept in receptacles with characteristic shapes (Figure 1), made of stone (alabaster, hematite, and marble), ceramic, wood or reed (Vandier D'abbadie, 1972). These receptacles had been placed in tombs as burial artefacts. Previous studies have shown that the make-up was used since the earlier periods (around 4000 BC for the pre-dynastic times) in relation to its aesthetic, hygienic, therapeutic and religious functions (Lucas and Harris, 1963; Jonckheere, 1952).

Since the time of the Old Kingdom (2700-2200 BC), cosmetics were used in religious ceremonies and can be found on lists of funeral gifts alongside various unguents (Ziegler, 1993). Their role is described in documents concerning religious worship, where the priest can be seen offering to the gods two small purses containing green and black make-up. Their function is respectively to "clean" the god's face and to enable him to "see through Horus's eye" (Moret, 1902; El-Kordy, 1982; Troy, 1993). These documents also describe the symbolic role that the ancient Egyptians attributed to cosmetics in maintaining cosmic order. They believed that the moon's cycle manifested the combat between Horus and Seth, i.e. the combat between light and darkness. According to this myth, Seth injured Horus's eye, thus endangering the return of the full moon. In order to stop the onset of destruction and restore the cosmic order ordained by the gods, the eye had to be cured, that is to say "made complete, rebuilt, given back its various elements". The well being of eyes was therefore assured by the power of cosmetics, whose function was to "make the eyes festive, make them shine, perfect them, make them radiate with life". In the same way that cosmetics filled and restored the eye of Horus and those of the dead, the everyday use of cosmetics had prophylactic and therapeutic functions.

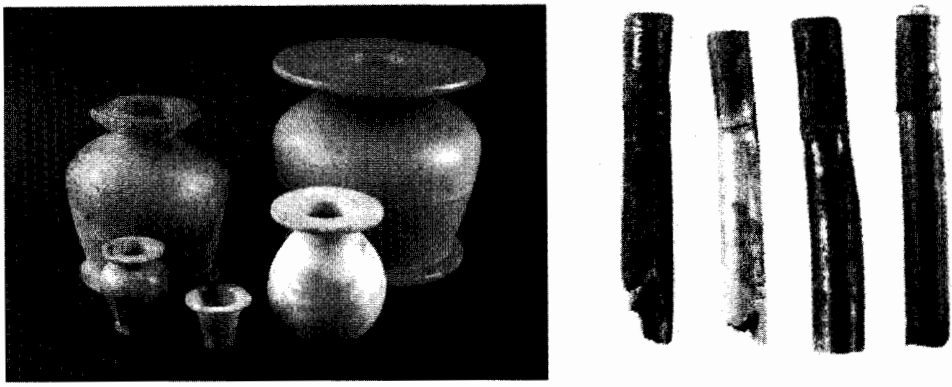

Figure 1. Photographs of make-up vases and reeds at Le Louvre museum

1.2. Description of the cosmetic powders

Analysing cosmetics to uncover their components and the way in which they were made is not a new idea. At the end of the 19th century, several researchers discovered that ancient Egyptians used a wide variety of very complex make-ups, which were very often lead-based compounds. Galena (lead sulphide), cerussite (lead carbonate), pyrolusite (manganese dioxide), chrysocolla (hydrated copper silicate) and malachite (copper carbonate) had also been identified by microscopy and micro-chemical analysis in more than one hundred samples (Lucas and Harris, 1963; Barthoux, 1926).

Our observations have been extended over small volumes of powder taken from 65 artefacts conserved in the Louvre Museum (Paris, France). A representative number of cosmetic mixtures, of different colours (white, grey, green or black) and different textures (hard, powdery or greasy), was examined by electron microscopy and X-ray diffraction. These specimens constitute an outstanding collection dated from the New Kingdom (1552-1070 BC), from the Middle Kingdom (2134-1650 BC), as well as from the Archaic period (3100-2700 BC). Part of the investigated samples come from the French excavations at the end of the 19th century, especially from the tombs near Deir-el Medineh (1550-1300 BC), a craftsmen's village near the Kings and Queens valleys in Middle Egypt. The archaeological context of some objects is well defined: for example, five reed cases (inv. E11048 a,b,c,d,e) were found in the excavations of Lady Touti's tomb at Medinet el-Gorab (Fayoum) in 1900 (Chassinat, 1901). Her death dates back to the 18th dynasty, just before or during Tutankhamun's reign. One reed case bears a column of hieroglyphs written with black ink, which describes the content as being a "3-stars" genuine mesdemet. The word "mesdemet" often refers to galena and the hieroglyph, which stands for "high quality", is here repeated three times. In addition to these boxes, the funerary furniture contained statues of women sitting near a toilet bag containing a mirror, an eye-shadow spoon, unguent boxes and hairpins.

Thus we identified the various as-found materials and worked out their combinations and respective proportions. The ultimate goal is to link the recipes with some possible specific properties and with the historical and archaeological records.

2. EXPERIMENTAL DETAILS

The samples were first observed under a scanning electron microscope (SEM) to observe the morphology and the elementary chemical composition of the grains of the powder (Philips XL30CP microscope equipped with a Si(Li) detector able to detect elements as light as carbon). The analysis by microscopy greatly helped to identify the chemical phases and brought to light the presence of lead compounds of sulphur, carbon, oxygen and chlorine. The various mineral phases were identified using the laboratory diffractometer Brüker D5000 ($\lambda_{CoK\alpha}$ =1,7903 Å) in Bragg-Brentano geometry, the powder being deposited on a flat sample holder made of silicon. The DiffractPlus programme (Socabim, 1998) was used for the qualitative analysis of the phases. The experimental diagram from each archaeological sample was compared with those of the single-phase reference samples available through the database

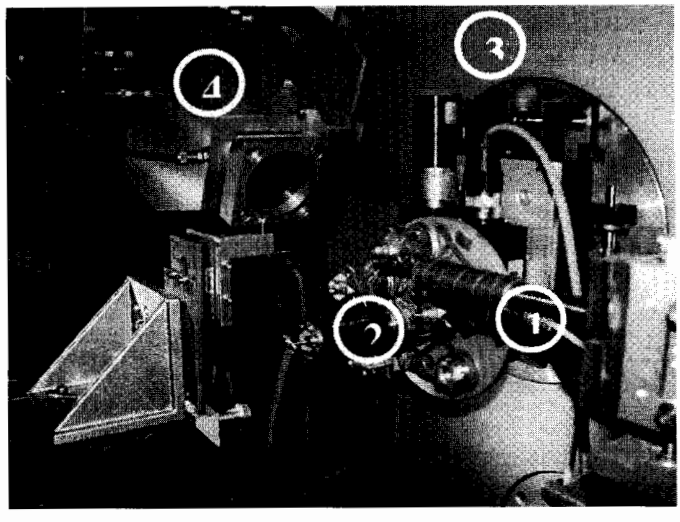

Figure 2. Photograph of the BM16 diffractometer. (1) X-ray beam exit collimator ; (2) goniometer head on sample holder ; (3) ω circle ; (4) detector and analyser crystal assembly.

maintained by the Joint Committee on Powder Diffraction Standards (in 1995, the JCPDS database contained 60,000 references).

Powder diffraction using synchrotron radiation was carried out at the DW22 line in the Laboratoire pour l'Utilisation du Rayonnement Electromagnetique (LURE), Orsay, France, and at the BM16 line at the European Synchrotron Radiation facility (ESRF), Grenoble,

France. The powder was placed in a capillary tube 300• m or 400• m in diameter used in transmission in the Debye-Sherrer geometry. At the beamline BM16, the diffractometer is designed for mounting various detectors and different sample environments (Figure 2). The present set-up used a nine-crystal analyser stage (nine scintillation counters, each fitted with a Ge(111) crystal and offset by ~2° with respect to one another) (Hodeau, 1999). The sample continuously spins on the axis of the diffractometer. Data are collected in a continuous scanning mode. This eliminates the dead time of a conventional step scan. Following data collection, the counts from the nine detectors are summed and normalised, to give the equivalent normalised step scan.

The advantages for this study by synchrotron radiation compared to conventional laboratory diffractometry are:

1) the wavelength is well adapted to the highly absorbing lead-based compounds, off the L-absorption edges of lead (see Table 1 and Figure 3);

Table 1
Linear absorption coefficient of galena (PbS), a major component of archaeological make-up, versus the wavelength used.

		wavelength (Å)	μ_{PbS} (μm^{-1})
D5000	flat plate holder	1.7903	0.233
LURE	capillary ∅400 µm	0.9627	0.0466
ESRF	capillary ∅300 µm	0.3532	0.0129

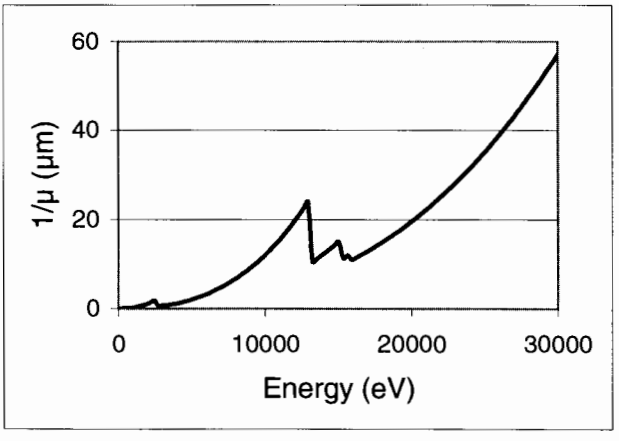

Figure 3. X-ray attenuation length for galena as a function of the photon energy

2) the high photon flux on the specimen ensures high statistics and a good signal-to-noise ratio within a reasonable counting time; at the ESRF, the magnitude of the most intense peak of a major phase can reach up to 30,000 counts in 4 hours (Figure 4). By coupling the

detectors with the analyser crystals, the signal-to-background ratio is improved, and trace compounds can be identified, and sometimes weighed.
3) the parallel beam optics combined with a Si(111) double-crystal monochromator and the post-sample Ge(111) analyser crystals of BM16 reduces the instrumental broadening and the diffraction pattern is immune to common aberrations (2θ error, sample misalignment) (Fitch, 1996). The instrumental contribution to the full width at half maximum (FWHM) around 10° 2θ is of the order of 0.003° 2θ for BM16. The high resolution was needed for interpreting the diagrams of some samples which could contain as many as 10 distinct phases. The high resolution was also advantageous for analysing the pure diffraction line profile after removal of the instrumental function.

3. DATA ANALYSIS

3.1. The Rietveld refinement of powder diffraction patterns

This method is the most efficient way of analysing X-ray and neutron diffraction patterns from powder samples when the crystal structures of the constituent phases are known (Rietveld, 1969). Rather than taking the integrated intensities of a few intense individual Bragg peaks, the full pattern profile is fitted using the instrumental function parameters, the structural parameters (lattice parameters, element scattering form factors, atomic positions and atomic displacement parameters) and the micro-structure parameters defining the sample peak profiles.

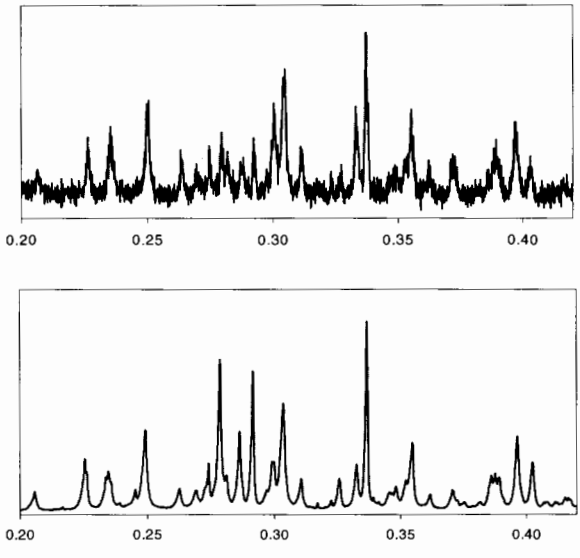

Figure 4. The high photon flux on the specimen ensures high statistics and a good signal-to-noise ratio within a reasonable counting time; at the ESRF, the magnitude of the most intense peak of a major phase can reach up to 30,000 counts in 4 hours

The Rietveld refinement program aims at minimising the following function:

$$M = \sum_i w_i (y_i - y_{ci})^2$$

W_i the weight of the intensity y_i measured over the i^{th} step of the diagram
y_{ci} the corresponding calculated intensity.

M is minimized using either the least-squares (whereby $w_i = \frac{1}{y_i}$) or the maximum-likelihood ($w_i = \frac{1}{y_{ci}}$). The intensity at the step i is calculated by adding the continuous background and the contribution of all the peaks which overlap at that point:

$$y_{ci} = y_{bi} + \sum_{\phi=1}^{N} S_\phi \sum_{k=k1}^{k2} j_{\phi,k} LP_{\phi,k} O_{\phi,k} M \left|F_{\varphi,k}\right|^2 \Omega_{i,\varphi,k}$$

y_{bi} the intensity of the continuous background at the position $2\theta_i$, obtained by linear interpolation
S_ϕ the scale factor proportional to the mass fraction of the phase ϕ
j_k the multiplicity of the $k^{ième}$ reflection
LP_k the Lorentz and polarisation factor
O_k the correction term which takes into account a possible preferred orientation, i.e. the difference with respect to an uniform, random orientation distribution of the constituent particles
M the correction term which accounts for any possible absorption and/or micro-absorption effects
$|F_k|$ the structure factor (including the thermal and disorder Debye-Waller terms)
Ω_{ik} the analytical function which best fits the instrument and sample diffraction peak profile

The summation in y_{ci} is carried out over every single crystalline phase present and over all the neighbouring reflections, k_1 to k_2, which contribute into the i^{th} step. The validity or the figure of merit of the profile fitting is estimated through a number of reliability factors R. Figure 5 shows the Rietveld refinement for the archaeological sample E11048e.

3.2. Quantitative analysis by the Rietveld refinement method

The quantitative analyses are based on the fact that the intensity diffracted by a crystalline phase is basically proportional to the quantity of matter irradiated (although in fact absorption effect corrections are required when the mixture contains compounds with highly contrasted absorption coefficients or different grain sizes). Archaeological samples are too precious for the internal standard method to be considered. Another most used method for quantitative analysis is based on the Reference Intensity Ratio (RIR). This consists in comparing the intensity of the most intense Bragg reflection of each of the phases present in the sample with the (113) reflection of corundum. However this technique is extremely

sensitive to systematic errors, especially those due to preferred orientation. On the other hand, using profile refinement techniques makes it possible to minimise the influence of texture, since they apply to the whole pattern and thus provide a more reliable quantitative analysis. In Debye-Scherrer geometry, one shows :

$$S_\phi \infty \frac{m_\phi}{(ZMV_c)_\phi}$$

m. mass of the phase present in the sample
Z. number of formula units per unit cell
M. mass per formula unit (often the molecular mass of the phase $_f$
V_c. volume of the unit cell

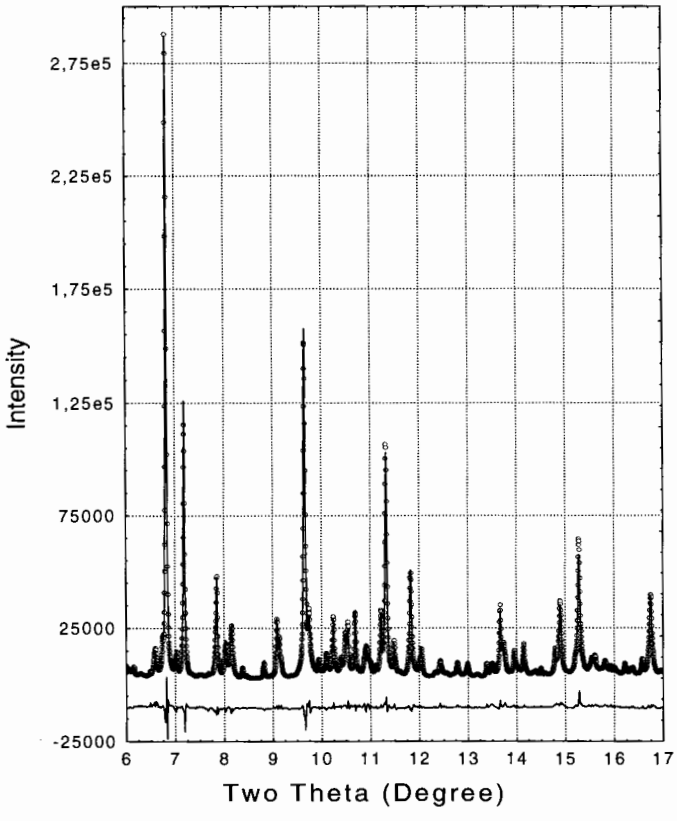

Figure 5. Observed (dots), calculated (solid line) and difference (bottom line) patterns of the archaeological sample E11048e

By constraining the sum of the mass fractions *W.* of all the phases present to be equal to unity, one gets :

$$W_\phi = S_\phi \frac{(ZMV_c)_\phi}{\sum_{\phi=1}^{N} S_\phi (ZMV_c)_\phi}$$

The same result could also be obtained from a measurement in the Bragg-Brentano geometry, given the area of the sample be larger than the beam footprint during the whole acquisition. This condition is not often fulfilled when examining small volumes of archaeological powder. The accuracy of the parameter *S.* (and hence • .) can be estimated from the standard deviation. The applicability and the advantages/limits of the Rietveld procedure were the case of study of the last Round Robin started in 1996 by Madsen, Hill, Groleau and Cranswick. Many Rietveld-type packages are commonly available ; the present study used the Fullprof programme (Rodriguez-Carjaval, 1990). The diffraction peaks were satisfactorily fitted by means of the pseudo-Voigt function convoluted with a correction function which takes into account the low-angle asymmetry caused by the axial divergence of the beam (Finger et al., 1994). Reference mixtures whose composition and granulometry were close to those of the archaeological samples were used to validate our protocol of measurement and our quantitative analysis.

The high resolution patterns collected at the ESRF on géological galena powders show some anisotropy of the peak profile, particularly along the planes h00 et h11 (Martinetto et al., 2000). The anisotropic peak profile was taken into account in the refinement, by using three different sub-sets of pseudo-Voigt function parameters. The preferred orientation along the clivage plane h00 was also often to be corrected.

Each archaeological powder is a mixture of compounds with highly different absorption coefficients (at • = 0.3532• , • can differ by two orders of magnitude). Hence micro-absorption corrections have to be taken into account in the quantitative analysis. These corrections are applied indirectly by dividing by the factor • the molar masses of the unit cell of the phases concerned. • provides for the absorption contrast according to Brindley's model (Brindley, 1945). The validity of these corrections was tested using reference mixtures made of lead compounds (PbOHCl) and alumina (Al_2O_3). The results obtained for the various mixtures, with and without corrections, are given in Table 2.

The effect on the diffracted intensities of the presence of a wide range of grain sizes within a sample was tested using the archaeological sample E20514. This powder contains a considerable quantity of large-grained galena (grain size • 50 • m) while the other phases of the sample have a much smaller grain size (as small as 1-5 • m for the synthesised lead chlorides). A sample of the powder was ground to obtain a homogeneous mixture of fine grains and Table 3 shows the relative results. The mass fractions of galena in the original powder had been under-estimated by roughly 10%, which illustrates that micro-absorption does occur within the powder. For shorter wavelengths, micro-absorption correction analysis shows that the errors induced in the mass fraction of lead compounds are generally small, less than 10%. The mass fractions of non lead-based compounds are liable to induce greater error than this, however such compounds are found only in minute quantities in the mixtures under consideration. In the rest of the present article, micro-absorption corrections will no longer be taken into account for the archaeological samples. The accuracy of the relative mass fractions

of the various compounds in man-made powders would seem sufficient to describe the recipes.

Table 2
Quantitative analysis of reference powder mixtures at $\lambda = 0{,}9627$Å.

	Mass fractions (%) weighed	Mass fractions by Rietveld no correction	Mass fractions corrected	μ (μm^{-1})	Mean grain size (μm)
Galena	50	46	-	0.0466	5
Laurionite	50	54	-	0.0365	2.5
Galena	95	94	-	0.0466	5
Laurionite	5	6	-	0.0365	2.5
Laurionite	80	78	80	0.0365	2.5
Alumina	20	22	20	0.0031	1.5
Laurionite	20	14	16	0.0365	2.5
Alumina	80	86	84	0.0031	1.5

Finally, in order to verify that the sample taken from the powder was representative of the whole container and also to check that the analyses were reproducible, two samples were taken from two different parts of the receptacle E20514 to be analysed and compared. The results, given in Table 3, show good agreement for the two different samples and the different analyses.

Table 3
Mass fractions of 2 samples of one cosmetic powder dated from the New Kingdom, independently measured at the LURE and at the ESRF in distinct capillaries.

# item		λ (Å)	PbS	$PbCO_3$	$Pb_2Cl_2CO_3$	PbOHCl	$PbSO_4$	ZnS	$ZnCO_3$
E20514	LURE	0,9620	73	3	9	1	6	6	2
E20514	ESRF	0,4134	72	2	9	2	4	9	2
E20514 ground	ESRF	0,4134	79	2	7	2	3	6	2

3.3. X-ray diffraction line profile

In complement to the qualitative and quantitative analyses, it is important to gain some information concerning the preparation method of some of the present constituent minerals. Some compounds are expected to differ by their microstructure, since the size and deformation of the grains depend on the processing of the powder. Such information can be inferred from the analysis of the diffraction line broadening, and more generally from the diffraction line profile, combined with SEM observations. The microstructure is essentially governed by two effects (Warren, 1969):

- the finite size of the coherently diffracting domains (also called crystallites) inside the grains ;
- the distortions (or micro-deformations) which cause an inhomogeneous strain of the atomic lattice and local shifts of the atomic positions with respect to the lattice nodes.

A common procedure is to fit the background with a spline or a polynomial function and the diffraction peaks with some adequate analytical functions (Langford et al., 1986). The lorentzian L, gaussian G, Voigt V, or pseudo-Voigt pV profiles are the most often used :

$$V(x) = L(x) * G(x) = \frac{1}{\beta_G} Re\left[erf\left(\frac{\sqrt{\pi}}{\beta_G} x + i \frac{\beta_L}{\beta_G \sqrt{\pi}} \right) \right]$$

where β_G et β_L respectively are the gaussian and lorentzian components of the integral breadth β, which is defined as the ratio of the integrated area of the peak over its height.

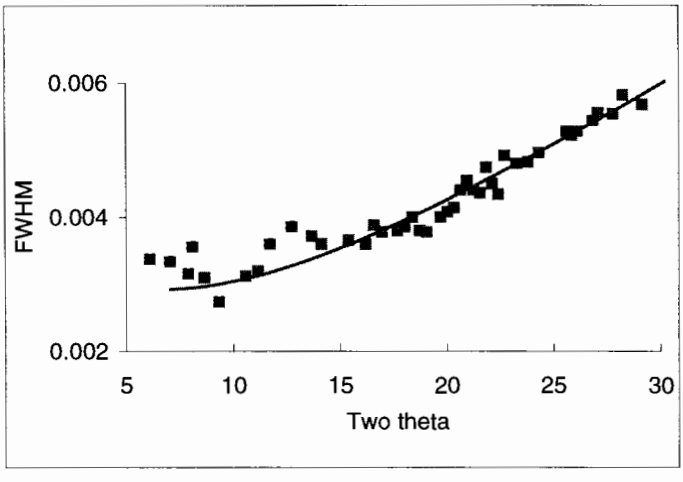

Figure 6. Instrumental Resolution Function of BM16 : Sabine's model (solid line) and FWHM of $Na_2Ca_3Al_2F_{14}$ diffraction lines (data points) at λ = 0.35 Å.

$$pV(x) = \eta L(x) + (1-\eta) G(x) = \eta \left(\frac{2}{\pi H} \frac{1}{1 + \frac{4}{H^2} x^2} \right) + (1-\eta) \left(\frac{2}{H} \sqrt{\frac{\ln 2}{\pi}} \exp\left(\frac{-4 \ln 2}{H^2} x^2 \right) \right)$$

where H is the full width at half maximum (FWHM) of the peak and η the mixing parameter.

Each individual observed peak $h(2\theta)$ was therefore fitted with a pseudo-Voigt function, convoluted with a function which accounts for the asymmetry caused by the axial

divergence of the beam (program PEAKOC, Masson,1998). The integral breadths β of the diffraction peaks, as well as the shape parameter • , and their variations with the Bragg angle are obtained. The parameters β and • , as obtained after refinement, are transformed into the corresponding Voigt parameters β_L and β_G (De Keijser et al., 1983). The instrumental correction of the observed data can then be made by a simple linear or quadratic subtraction of the lorentzian (cauchy) and gaussian widths of the instrumental function $g(2\theta)$ (Langford, 1992; Balzar and Ledbetter, 1993).

The FWHM of the instrumental profile $g(2\theta)$, also called the Instrumental Resolution Function (IRF), was estimated by measuring the diffraction peaks of two reference materials : NIST SRM660 LaB_6 and $Na_2Ca_3Al_2F_{14}$ in experimental conditions analogous with those for the measurement of the archaeological specimens. The sample broadening of the standard $Na_2Ca_3Al_2F_{14}$ is neglegible with respect to the instrumetal broadening. The measured width of g (IRF) can then be compared with the analytical curve given by Sabine (1987), taking into account the vertical divergence and the angular acceptances of the monochromator and analyser crystals (Figure 6). Both the experimental FWHM of the standard peaks and the theoretical curve agree well, and the IRF can be calculated at any 2θ.

The simplified methods of integral breadths use several orders (at least 2) of reflection from one particular family of planes, in order to separate the size and strain effects. . They are based on the principle that:

- the size effect does not depend on the order of reflection
- the lattice strain effect does depend on the order of reflection

Furthermore, the sample-broadened profile f being the convolution of the size and micro-deformation profiles, the type of line profile of each effect must be defined beforehand so that a function linking the integral breadth • to the micro-structural parameters can be established (Klug and Alexander, 1974). One usually assumes that either the size and strain profiles are lorentzian (Cauchy) (L-L), or both are gaussian (G-G) or alternatively the size profile is lorentzian and the strain profile is gaussian (L-G):

$$\beta_f^* = \frac{1}{<D>_v} + 2ed^* \qquad (L-L) \qquad \text{with } \beta^* = \beta\frac{\cos\theta}{\lambda}$$

$$\beta_f^{*2} = \frac{1}{<D>_v^2} + 4e^2d^{*2} \qquad (G-G) \qquad d^* = \frac{1}{d} = 2\frac{\sin\theta}{\lambda}$$

$$\beta_f^* = \frac{1}{<D>_v} + 4e^2\frac{d^{*2}}{\beta^*} \qquad (L-G)$$

The slope and the intercept at zero of the curve • . (d^*) yield respectively the volume-averaged size of the crystallites $<D>_v$ and the upper limit e of the micro-distortion (Williamson and Hall, 1953).

Alternatively some methods make use of the overall peak profile. They are more accurate and do not rely on any assumption as the analytical shape of the profile does. They intrinsically contain some information on the spatial and frequency distribution of the size and strain, but their application often suffers some approximations and are more computer-

demanding (Warren and Averbach, 1950). These methods also are limited whenever the peaks overlap with neighbouring reflections, as is often the case in the diagrams of archaeological powders. If the precise form of the Bragg reflection is needed, the Stokes deconvolution method is usually used (Stokes, 1948). This consists of expanding the instrumental profile g and the observed Bragg peak h into their Fourier series as a function of L, where L is the distance perpendicular to the diffracting planes. The Fourier coefficients of the true profile f are then obtained by the complex division of both coefficients at all L values.

4. RESULTS AND DISCUSSION

4.1. Phase identification

Three quarters of the products contain four lead-based main phases: the black galena and three white products, namely the cerussite PbCO3, the phosgenite Pb2Cl2CO3, and the laurionite PbOHCl (Figure 7). Galena and cerussite are well known lead ores which were abundantly mined in Ancient Egypt from mines situated along the Red Sea coastline (Castel and Soukassian, 1989). Galena being greyish back and cerussite white, various shades of grey could have been obtained simply by mixing them together.

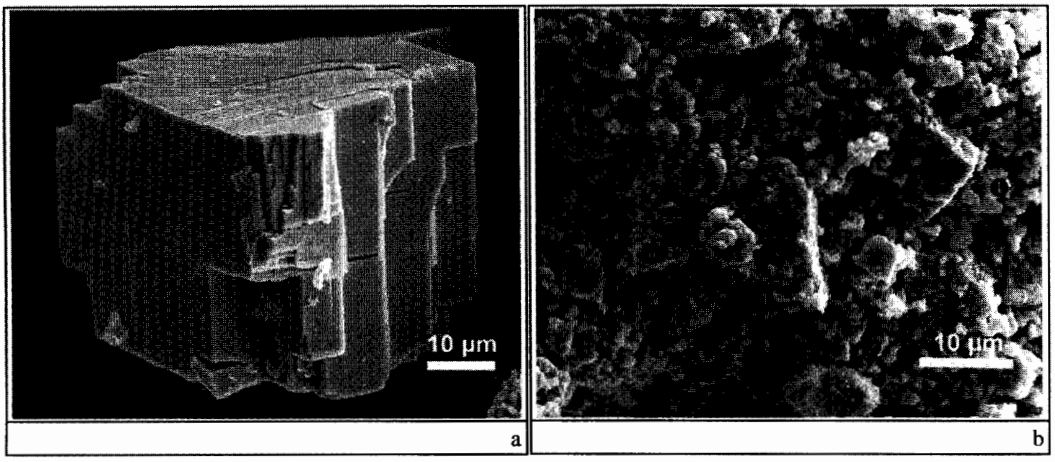

Figure 7. SEM micrographs of major mineral phases of Egyptian makeup powders. (a): Cubic crystal of galena with cleaved faces along (100). (b): Mineral mixture of (1) galena (cubic crystals of 10 to 20 µm long), (2) cerussite (tabular grains about 10 µm long) and (3) phosgenite (ovoid crystals of less than 1 µm long).

Both the phosgenite and the laurionite are white too and therefore cannot have been added to the mixture solely for questions of pigmentation. The on-going analysis brought to light the fact that the two latter chloride compounds could only have been prepared by means of wet chemistry before being incorporated into the mixtures in the form of fine white powders (Walter et al., 1999). Greco-roman authors of the first century AC described the way this

synthesis was carried out, and identified these compounds as health products for eyes and skin and for hair washing (Zehnacker, 1983; Wellman, 1958). These authors explained how the "purified silver foam" (lead monoxide in fact) was ground, then mixed in water with rock salt and sometimes natron (mainly sodium carbonates) and subsequently filtered. This process was repeated daily from one to six weeks. These chemical reactions have been repeated in the laboratory where lead monoxide powders were mixed with sodium chloride and sodium carbonate in water. The pH-pCl-pCO3 stability of the resulting lead-based products was observed at room temperature. Thus it was observed that these recipes give rise to a slow transformation of the weakly-soluble oxide, producing an alkaline solution whose neutrality (pH $\approx$ 7) was approximately maintained by the frequent renewal of the water. Under these conditions, both the laurionite and the phosgenite are formed in proportions which depend on the concentration of dissolved carbonates (Walter, 1999).

The variety of these mixtures and the presence of white synthesised products indicate that the ancient Egyptians deliberately made cosmetics with specific properties. In particular the lead chlorides must have been rather added for their remedial effects, which are in fact described in some ancient Egyptian manuscripts. For example the Ebers medical papyrus, dated around 1550 BC, associates cosmetics and medicine, giving recipes for dying hair, modifying the colour of the skin and beautifying the body (Bardinet, 1995). It gives detailed recipes for eye drops, masks and make-up for the eyes and eyelids which were to be prescribed to cure various ailments. Proportions were given as a percentage of a reference volume, with the relative proportion of some ingredients being as low as 1/64. Ninety-five recipes of cures for eye problems are described in this papyrus with a vocabulary which is usually associated with the application of cosmetics: "Make up the eyes with this ...", "Use this eye make-up in the evening...", "Make-up to improve the eye sight...". A certain amount of information concerning the texture of the mixture to be obtained, its qualitative or quantitative composition and how it is to be used can be obtained from the study of these texts. They all mention galena associated with other mineral and organic substances. It is essential that the translation of these recipes be reviewed. For example, in the translated recipe number 359 of the Ebers papyrus (Bardinet, 1995), the word galena appears three times, but each time the words associated with it are different:

Another (remedy) for eye care : galena :1 ; red ochre (tjerou) : 1 ; djaret-plant : 1 ; gesefen-galena : 1 ; male part of galena : 1. (This) is to be prepared as an homogeneous mass and applied onto the eyes.

In the light of the recent findings and working alongside Egyptologists, it may become possible to better understand the signification of the various modifiers used with galena in the hieroglyphs and thus produce a more accurate translation of the compounds. The same can be said in so far as laurionite and phosgenite are concerned. Neither of these names of minerals are quoted as such in the recipes, but perhaps they should be considered as a possible translation for the 'sia-mineral of the south' and the 'sia-mineral of the north' which are frequently associated with the word galena.

Since not all the seams of galena and cerussite mined were of the same quality, the ancient Egyptians must have sometimes encountered difficulties extracting the required pure compounds from the ore. Thus some traces of lead and zinc compounds, known for being oxidised galena ore, are found in the samples: anglesite $PbSO_4$, suzannite $Pb_4(CO_3)_2PbSO_4(OH)_2$, palmierite $K_2Pb(SO_4)_2$. Other minerals are also found in association with the Pb-Zn ore sources : sphalerite ZnS, smithsonite $ZnCO_3$, hemimorphite

$ZnSi_2O_7(OH)_2H_2O$). Even very tiny quantities of compounds typical of dolomite limestone can be found in the samples, which correspond to the rocks in which seams of lead ores can be found around the Red Sea: gypsum $CaSO_4$ $2H_2O$, dolomite $MgCO_3$, calcite $CaCO_3$ and quartz SiO_2. These elements coincide with data supplied by geological studies of the lead mines worked during the time of the Pharaohs (Castel and Soukassian, 1989). However, it should also be noticed that calcite could have originated from the walls of the receptacle when the sample was being taken, and that some of the quartz could have come from the pestles and mortars used to prepare some of the samples.

Finally, the presence of cotunnite $PbCl_2$ in five of the samples could be associated with the chemical preparation of the two synthesised compounds. Our laboratory experiments mimicking the production of laurionite and phosgenite show that the cotunnite can sometimes form in acid solutions with high levels of chlorine. It may be that this is an unintentional by-product of laurionite and phosgenite making process.

We have also been able to show that various quantities of fatty acids of animal provenance were added to the powders to vary their texture (Comparon et al., 1999). The proportions are fairly similar to the proportions of vegetable fats added to the make-up nowadays, and produce textures ranging from loose face powder, eye shadows to kohl eye pencils.

4.2. Phase proportions

Figure 8 shows the mass fractions of galena, cerussite and synthetic lead compounds (laurionite, phosgenite and contunnite) for 28 different powders on a ternary diagram. The other compounds, present only in minute or even trace quantities, have been ignored. As shown in section 4.1, they provide some information concerning the origin or the elaboration process of the make-up, but they do not seem to have played an important part in the recipes. In fact, the difficulty encountered is to classify each of the ingredients in order to find the typical recipes (if any) for a given period. The wide distribution of the cosmetic compositions is immediately obvious and no single group stands out as representative of a particular recipe or specific use. Some of the difficulty in interpreting the compositions also arises from the fact that the available archaeological corpus, which has been analysed, is not yet considerable enough.

A high percentage of galena is found in most of the mixtures and gives the powder a metallic-grey or black shade. However, in seven of the powders, there is less than 15% of galena and three do not contain any at all. This shows that very light grey or white products were also used alone. Such light colours do not seem appropriate for use as eye make-up and may rather have been used as foundation cream or face powder. The scene on a tombstone kept in the British Museum (BM 1658) which dates from the Middle Kingdom backs up this hypothesis. It shows Lady Ipouet holding a mirror in her left hand and a piece of cloth in her right, with which she seems to be applying make-up onto her face.

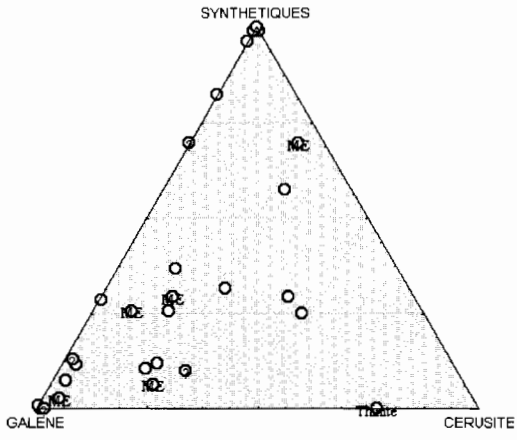

Figure 8. Diagram showing the mass fractions of galena, cerussite and synthetic compounds of 28 make-ups used in Ancient Egypt. The powders dated from the Middle Kingdom (NE) and from the Archaic period (Thinite) are indicated.

It can be seen that the synthetic products probably make their appearance at the time of the Middle Kingdom. They are found in all five samples, which date from that period whereas there is no evidence of these products in the sample from an earlier period. They were very much used since 86% of the powders analysed contains some laurionite and some phosgenite. When exactly these products appeared still has to be dated. The study of objects from the Old Kingdom and the Archaic period would make it clearer what led the Egyptians to prepare such compounds. Unfortunately, the remains of cosmetics from these periods are very rare and it would be most interesting to examine the objects kept in the Egyptian collections of other museums.

4.3. Conditioning of the cosmetic powders

Two minerals are particularly interesting: one is the galena, obtained by manual grinding of the natural ore, and the second one is the laurionite, made of fine grains and obtained by a chemical reaction in solution.

The analysis of the peak profile of archaeological galena (from the make-up numbered E20514) was compared with that of a geological galena powder mined in the United States which had been hand ground with a pestle and mortar, then passed through a 63-125• m mesh. The reflections corresponding to multiplets or overlapping with some reflections of other phases were identified and thus ignored in the analysis of the microstructure. The FWHM variation of the archaeological galena is given in Figure 9, and it is compared with the instrumental resolution function of beamline BM16. It can be seen that the galena is highly crystallised and produces only a very low broadening (of the order of 0.01° 2• FWHM, very close to the instrumental broadening). It is clear that this analysis can only be carried out on an instrument with a very high resolution. For comparison the IRF of a laboratory diffractometer exceeds 0.05° 2• FWHM. Figure 10 shows the integral width • of the

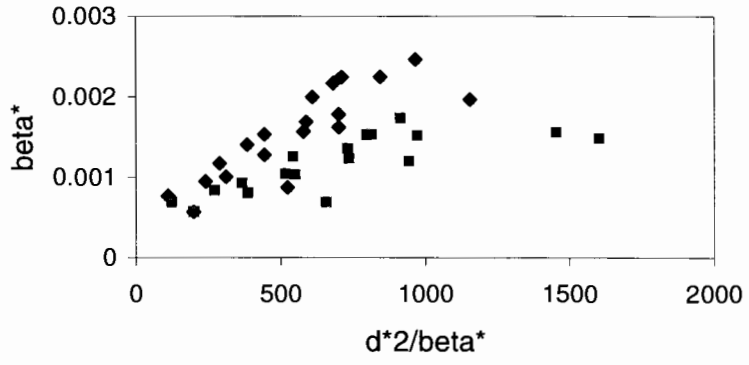

Figure 9. FWHM of archaeological galena (E20514) diffraction peaks, compared with the Instrumental Resolution Function of BM16 (solid line) and D5000 (dotted line).

broadened profiles, corrected for the instrumental contribution, on a Williamson-Hall L-G diagram (Equations in section 3.3).

Figure 10 shows a marked anisotropic broadening of the galena peak profile. This (hkl) dependency has already been mentioned in section 3.2 and was taken into account in the Rietveld refinements by separating the galena reflections into three groups, refined with different profile parameters. This anisotropy could be explained by the presence of a strain field associated with dislocations, and is being modelled by introducing a contrast factor

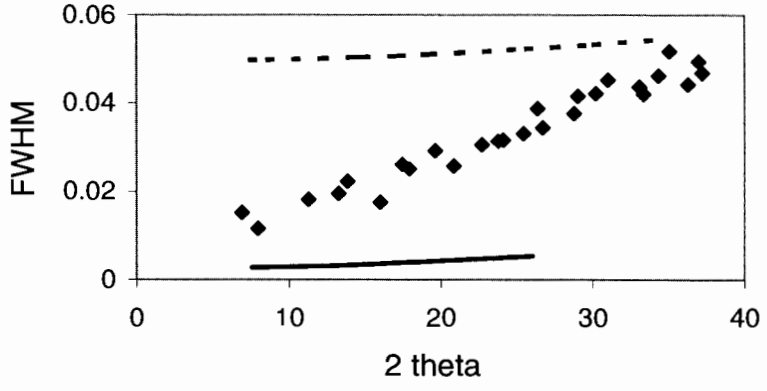

Figure 10. Williamson-hall diagram in reciprocal space (by the method of integral breadth using equation of section 3.3): the FWHM of archaeological (lozenges) and geological (squares) galena powders.

Figure 11. Senynefer and his wife (New Kingdom, 18th dynasty, ~1410 BC.). (H: 68, W:85, Museum Le Louvre E27161). Copyright RMN- Chuzeville

which depends both on hkl and on the elastic constants of the material (Klimanek, Kuzel, 1988; Ungar, Borbély, 1996). Leaving this anisotropy aside, the integral width method, applied to the individual peaks of galena, gives a crystal size of the order of 2000Å for both samples and an upper deformation limit of 0.05% for the geological sample. The archaeological powder shows a greater lattice deformation than the geological powder and therefore it may have been more finely ground. This hypothesis would seem to be confirmed by the SEM observations, which show the E20514 galena sample forming a more heterogeneous assembly of small cubes ranging from 20• m to 150• m long, with a significant fraction of smaller grains. The analysis of other archaeological galena powders show that the galena was more or less finely ground by the Egyptians to obtain either a black mat powder, or grey powders with metallic overtones. The larger the grains of galena, the brighter and the more reflecting they are. The different make-up obtained in this way may have been destined for use on different parts of the eye. It is easy to imagine that the finer mat powders, applied inside the lower eyelid, would adhere thanks to the humidity of the eye itself. The powder made of coarser grains would have to be held by an organic binding agent and would be more likely to be placed in a thick coat on the upper eyelid (Figure 11).

The archaeological laurionite powder AF143 has also been processed and its microstructure compared with that of the newly synthesised powder described in section 4.1 (Figure 12). The mixing parameter • of the pseudo-Voigt function is of the order of 0.8 for the galena powder E20514 and of the order 0.2 for the laurionite powder AF143. Therefore

the origins of the peak broadening are obviously very different for the two minerals. Only the size effect contributes to the peak broadening of the laurionite pattern, whereas both size and strain effects are present in the galena diffraction lines. Both the archaeological and the synthetic laurionite powders have similar behaviour and their crystal size can be evaluated at 1000Å. The scanning electron microscopy study of these powders show that the laurionite is composed of small grains, of about 1μm, which matches the evaluated size. The absence of any significant lattice distortion in the archaeological laurionite and its identical behaviour to that of the synthesised powder reinforces the hypothesis of the chemical process of preparation of this Pb-Cl compound. The synthetic powders, obtained in the form of very fine powders, would simply have had to be mixed with the previously ground mineral powder.

The case of galena and laurionite have illustrated the information which can be obtained from the analysis of diffraction peak broadening. Such analyses should shortly be applied to other compounds found in the cosmetic powders from Ancient Egypt. Furthermore, a more detailed study is being carried out at present, based on the interpretation of the overall peak profile by Fourier analysis.

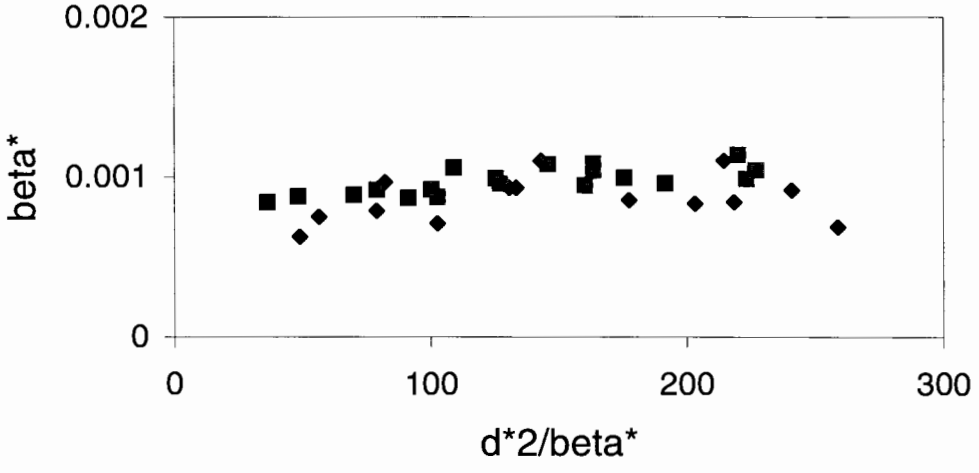

Figure 12. Williamson-hall diagram in reciprocal space (by the method of integral breadth using equation of section 3.3): the FWHM of synthesised (lozenges) and archaeological (squares) laurionite powders.

5. Conclusion

The analysis of cosmetics as used in Ancient Egypt reveals the great variety of compositions using lead compounds and an advanced know-how in chemical synthesis. This shows that 4000 years ago, people already wanted more impact from their use of cosmetics than simply highlighting of the eyes. This work shows the benefits of combining optical and electronic

microscopy methods, X-ray fluorescence measurements and ion beam analysis (Proton-Induced X-ray Emission, Rutherford Backscattering Spectrometry, Nuclear Resonance Analysis) with X-ray diffraction in view of identifying and weighing the crystalline phases in archaeological or artistic objects. The use of X-ray synchrotron radiation enables one to examine small volumes of rare and precious, highly X-ray absorbing powders, without any alteration prior to the analysis. The high resolution and high signal-to-background ratio make it possible to determine the composition of complex mixtures, particularly when the specimen is composed of a large number of phases or when some ingredients are present in extremely small proportions (< 1%). The analysis of the Bragg line profiles could also provide some insight into the micro-structure of some minerals (size and distortions of the grains), in relation with the preparation of the make-up (synthesis, grinding, sieving).

Acknowledgements: this research was carried out in collaboration with L'Oréal Recherche and has benefited from the support of the Département des Antiquités Egyptiennes of Le Louvre museum.

REFERENCES

Balzar D. and Ledbetter H., J. Appl. Cryst., 26 (1993) 97.
Bardinet T., Les papyrus médicaux de l'Egypte pharaonique, Fayard, Paris, 1995.
Barthoux J., Les fards, pommades et couleurs dans l'Antiquité. Congrès Int. de Géog., Le Caire, Avril 1925, No IV (1926) 251.
Brindley G. W., Phil. Mag., 36 (1945) 347.
Castel G. and Soukassian G., Gebel el-Zeit I. Les mines de Galène, Fouilles de l'IFAO, No XXXV, Le Caire, 1989.
Chassinat E., Bull. Inst. Fr. Arch. Orient., 1 (1901) 225.
Comparon C., Bernard T., Manzin V. and Kaba G., J. High Resol. Chromatogr., 22 (1999) 635.
de Keijser T. H., Mittemeijer E. J. and Rozendaal H. C. F., J. Appl. Cryst., 16 (1983) 309.
El-Kordy Z., L'offrande des fards dans les temples ptolémaïques. Annales du service des antiquités de l'Egypte, No LXVIII (1982) 195.
Finger L. W., Cox D. E. and Jephcoat A. P., J. Appl. Cryst., 27 (1994) 892.
Fitch A. N., Mater. Sci. Forum, 219 (1996) 228.
Hodeau J-L., Bordet P., Anne M., Prat A., Fitch A.N., Dooryhée E, Vaughan G., Freund A., SPIE Conference on Crystal and Multilayer Optics - San Diego,1998. Proceedings SPIE, 3448 (1998) 353.
Jonckheere F., Histoire de la médecine, 7 (1952) 2.
Klimanek P. and Kuzel Jr. R., J. Appl. Cryst., 22 (1988) 299.
Klug H. P. and Alexander L. E., X-ray Diffraction Procedures for Polycrystalline and Amorphous Materials 2nd ed, Wiley, New York, 1974.
Langford J. I., Accuracy in Powder Diffraction, NIST Spec. Pub. No 846 (1992) 110.
Lucas A., Harris J.R., Ancient Egyptian Materials and Industries, Edward Arnold Ldt., London, 1963.
Martinetto P., Anne M., Dooryhée E. and Walter P., Mater. Sci. Forum, 321-324 (2000) 1062.
Masson O., Thèse de l'Université de Limoges, France, 1998.
Moret A., Le rituel du culte divin journalier en Egypte, Paris, 1902.

Rietveld H. M., J. Appl. Cryst., 2 (1969) 65.
Rodriguez-Carjaval J., Abst. Satellite Meeting on Powder diffraction of the XVth IUCR Congress, No 127 (1990).
Sabine T.M., J. Appl. Cryst., 20 (1987) 173.
Stokes A. R., Proc. Phys. Soc. Lond., 61 (1948) 382.
Troy L., Bull. D'Egyptologie, No 106/1 (1993) 351.
Ungár T. and Borbély A., Appl. Phys. Lett. 69 (1996) 3173.
Vandier d'Abbadie J., Catalogue des objets de toilette égyptiens du Musée du Louvre, Réunion des Musées Nationaux, Paris, 1972.
Walter P., L'actualité chimique, No Novembre (1999) 134.
Walter P., Martinetto P., Tsoucaris G., Bréniaux R., Lefebvre M.A., Richard G., Talabot J. and Dooryhée E., Nature, 397 (1999) 483.
Warren B. E., X-ray diffraction, Addison-Wesley, New York, 1969.
Warren B. E. and Averbach B. L., J. Appl. Cryst., 21 (1950) 595.
Wellman M., Dioscoridis Pedanii, De Materia Medica, libri quinque, Weidmannsche Verlagsbuchhandlung, Vienna, 1958.
Williamson G. K. and Hall W. H., Acta Metallurgica, 1 (1953) 22.
Zehnacker H., Pline l'Ancien, Histoire naturelle, livre XXXIII, Les Belles Lettres, Paris, 1983.
Ziegler Ch., Le Mastaba d'Akhethetep, une chapelle funéraire de l'Ancien Empire, Réunion des Musées Nationaux, Paris, 1993.